Morphology of block copolymers and mixtures of block copolymers at free surfaces*

Hirokazu Hasegawa and Takeji Hashimoto†
Department of Polymer Chemistry, Faculty of Engineering, Kyoto University, Kyoto 606, Japan
(Received 25 December 1990; revised 22 January 1991; accepted 24 January 1991)

The microdomain morphology of block copolymers at the free surfaces of solution-cast films was investigated by means of transmission electron microscopy and ultramicrotomy. The free surfaces of block copolymers consisting of amorphous components obey the thermodynamic requirements, i.e. the constituent block chains with lower critical surface tension always cover the free surface even for block copolymer films in which the component with higher critical surface tension forms the matrix. On the other hand, the free surfaces of block copolymers with crystalline components are governed by the crystallization kinetics, and their morphology depends on the orientation of the crystalline lamellae near or at the free surface. Therefore, the surface composition may vary with the method of preparation, and both amorphous and crystalline components can have a chance to be exposed to the free surface.

(Keywords: block copolymer; transmission electron microscopy; ultramicrotomy; free surface; morphology; microdomain structure)

INTRODUCTION

The morphology of block copolymers and their blends at surfaces and interfaces is an interesting subject to study. Many investigators have studied this subject with various techniques[1–5]. The most direct approach to this problem is the direct observation of the free surfaces or interfaces by electron microscopy, which enables one to look at the microdomain structure typically of the order of several tens of nanometres. We previously reported an effective technique to observe cross-sectional views of the free surfaces of cast films of block copolymers and the preliminary results in a short communication[1]. This is the full paper of that study.

EXPERIMENTAL

Poly(styrene-*b*-isoprene) (SI) and poly(styrene-*b*-butadiene) (SB) block copolymers were synthesized by sequential living anionic polymerization using s- or n-butyllithium as the initiator and benzene or tetrahydrofuran (THF) as the solvent. Although a number of SI and SB block copolymers were investigated in this study, the results were common to many samples. Therefore, we pick out in this paper only several samples that exhibit the typical morphologies, and the sample characteristics are given only for those samples in *Table 1*. Unless otherwise specified, SI and SB block copolymer samples were cast from 5–10% solutions in toluene at 30°C in Pyrex® Petri dishes for a time period of 1–2 weeks, and further dried in a vacuum oven for several days at room temperature. The Petri dishes were cleaned with an ordinary kitchen detergent, rinsed with distilled water and dried in an oven before film casting, but no other special treatment was carried out on them. The thicknesses of the cast films were 0.1–0.5 mm. Small test pieces (1 mm × 1 cm) for ultrathin sectioning were cut from the cast films, stained with osmium tetroxide vapour until staining was observed, and embedded in epoxy resin. The epoxy resin was prepared a long time in advance so that the polymerization proceeds to some extent, which is expected to prevent the swelling of the samples by the epoxy resin. Curing of the epoxy resin was done in a temperature-controlled oven at 50°C, which is far below the glass transition temperature of polystyrene, so that no structural rearrangement should be possible.

A multiblock copolymer[6,7] of nylon-6,10 and poly(propylene oxide) (PPO) with 56 wt% PPO content (sample code 61P3-56) was kindly supplied by Professors K. Sanui and N. Ogata, Sophia University, Tokyo Japan. The film specimen of the sample cast from a solution in *m*-cresol was used as received. Small test pieces

Table 1 Characterization of sample polymers used in this study

Sample code	Polymer[a]	$M_n \times 10^{-4}$	Weight fraction of PS	M_w/M_n
HY-12	SI diblock	52.4	0.52	1.16
HK-5	SI diblock	18.2	0.31	1.25
HS-11	SI diblock	85.0	0.80	1.31
HY-10	SI diblock	16.4	0.69	1.17
TOKI-12	SB diblock	9.99	0.52	1.03

[a]SI, poly(styrene-*b*-isoprene); SB, poly(styrene-*b*-butadiene)

* Presented in part at 1987 Fall Meeting of the Materials Research Society, Boston, December 1987
† To whom correspondence should be addressed

0032-3861/92/030475-13

of the film specimen for ultrathin sectioning were first stained with ruthenium tetroxide vapour, and embedded in poly(methyl methacrylate) (PMMA) resin.

The ultrathin sections of the film specimens that contain the cross-sectional views of the free surfaces were prepared with the technique previously reported[1] by using an LKB 4800A Ultrotome® with a glass knife at room temperature. Copper electron microscope grids of large mesh size (50 mesh per inch) with Formvar (polyvinylformal) supporting film coated with evaporated carbon were used to pick up the ultrathin sections so that the entire area of each ultrathin section can be observed. The carbon replicas of the free surfaces of the film specimens with platinum–palladium shadowing were also prepared for some of the block copolymer samples using a two-stage replica technique with triacetylcellulose film. Transmission electron microscopy was done with a Hitachi H-600S transmission electron microscope at 100 kV accelerating voltage. The morphology of block copolymers at the polymer–glass interface was also examined for some samples.

RESULTS AND DISCUSSION

For the sake of convenience, let us first define the Cartesian coordinates *Oxyz* with respect to the polymer–air or polymer–substrate interface as given in *Figure 1*. *Oz* is taken in the direction normal to the interface, while *Oxy* is taken in the plane of the interface. The coordinate was taken with respect to the average macroscopic interface as drawn by the full line. The interface varies locally as drawn by the broken curve and the unit vector l normal to the interface depends on the coordinates (x, y).

Block copolymers in their strong segregation limit exhibit microphase-separated structures with various morphologies depending on the copolymer composition, flexibility of the block chains, interfacial tension between the constituent chains and condition of sample preparation[8–10]. The microdomain morphology of AB block copolymers probably changes from A spherical microdomains dispersed in B matrix (hereafter denoted by S_A), to A cylindrical microdomains dispersed in B matrix (C_A), to A tetrapod network[8,11] in B matrix (T_A), to alternating lamellae of A and B (L_{AB}), to B tetrapod network in A matrix (T_B), to B cylindrical microdomains dispersed in A matrix (C_B) and finally to B spherical microdomains dispersed in A matrix (S_B) with increasing volume fraction of A component.

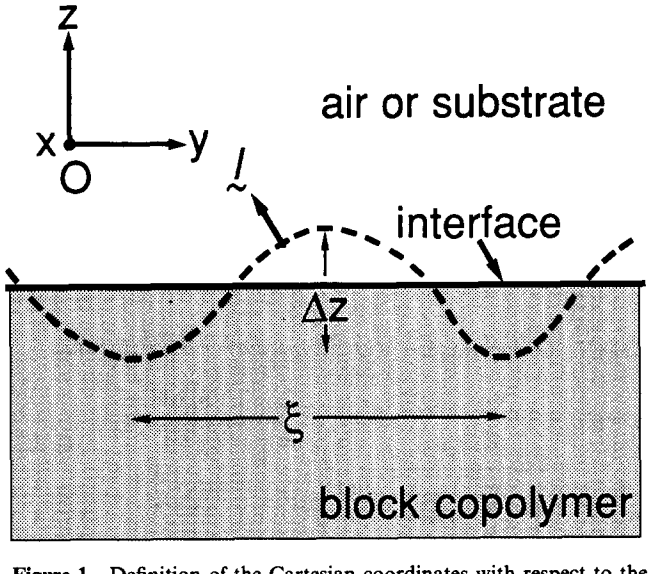

Figure 1 Definition of the Cartesian coordinates with respect to the polymer–air or polymer–substrate interface (full line). The local interface varies as drawn by the broken curve

The appearance of the free surfaces of as-cast films of SI and SB block copolymers depends strongly on their microdomain morphologies. According to our experience, it is sometimes possible to guess the microdomain morphology just by looking at the surfaces of cast films with the naked eye. In general, films with C_A and C_B morphology exhibit the roughest free surfaces, those with S_A and S_B morphology exhibit the smoothest free surfaces, and those with L_{AB}, T_A and T_B morphologies are in between. Here the surface roughness is referred to the variation Δz along the *Oz* axis in *Figure 1*. The persistence length ξ of this roughness Δz in any direction in the plane parallel to *Oxy* is largest for lamellar microdomains (order of centimetres to millimetres) and decreases in the order lamellar > cylindrical > spherical microdomains, ξ being of the order of 1 to 0.1 mm and 10 to 1 μm for the latter two morphologies. Krigbaum *et al.*[12] attributed the macroscopic hexagonal pattern formed on the free surfaces of styrene–butadiene–styrene (SBS) triblock copolymers cast from solutions to the Bénard effect, an ordering phenomenon of convection currents into cells during solvent evaporation. However, we consider that another interpretation is also possible: the surface patterns are related to local expansion and shrinkage of the domains in directions normal and parallel to their interface, caused by the increasing segregation power during the solvent evaporation process (grain-boundary relaxation in the unswelling process as discussed in Figure 9 of ref. 13). The deformation of grains composed of domains is strongly dependent upon direction for L_{AB}, C_A and C_B but less directionally dependent for S_A and S_B. During the solvent evaporation process, the segregation-driven deformation of films containing grain structure takes place with the constraint that one surface of the film is attached to the glass but the other surface is free, in contact with air. If this deformation is strongly directionally dependent, it may generate the macroscopic surface patterns as seen in the L_{AB}, C_A and C_B morphologies. If it is less directionally dependent, it may not generate the macroscopic pattern but rather a microscopic one as seen in S_A and S_B. Their free surfaces are as smooth as the homopolymer by observation with the naked eye.

In the previous paper[1] we showed that in the case of an SI block copolymer with L_{AB} morphology (L_{SI}), the polyisoprene (PI) component always occupied the free surface (the surface in contact with air during the film casting process) of toluene-cast film, regardless of the orientation of the lamellae with respect to the free surface. *Figure 2* shows an electron micrograph with such characteristic features observed over a more extended area than those shown in the previous paper[1] for an SI block copolymer (HY-12 in *Table 1*) with relatively large molecular weight ($M_n = 5.24 \times 10^{-5}$) and a lamellar morphology. In the micrograph the free surface of the block copolymer film can be clearly distinguished and is found at the interface between the sample film and the epoxy resin, the featureless embedding material attached only to the free surface (the upper part of the micrograph).

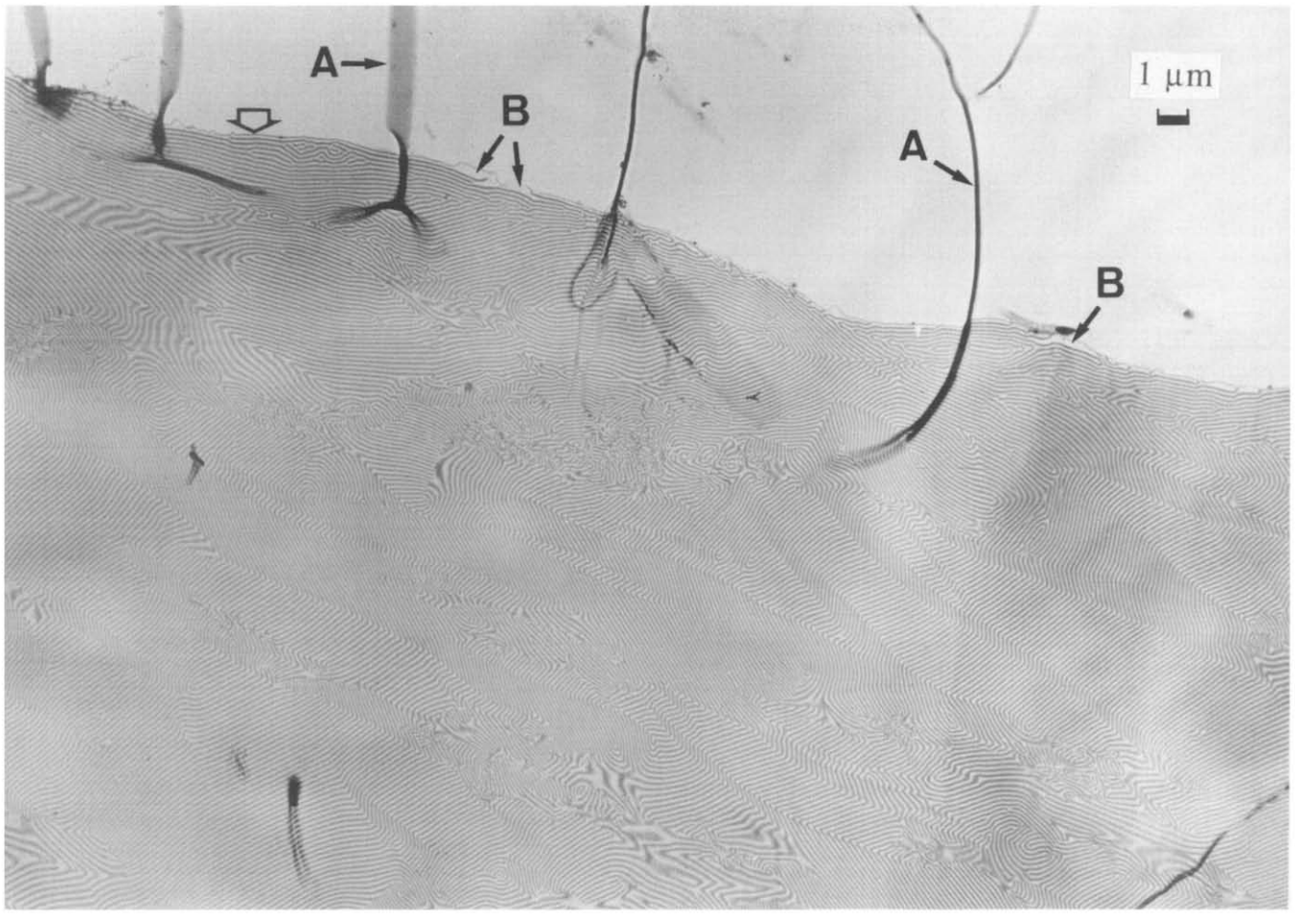

Figure 2 Electron micrograph of ultrathin section of HY-12 (SI) film cast from toluene solution and stained with osmium tetroxide. The upper part is epoxy resin, the embedding material, and the boundary between the epoxy resin and the sample film indicated by the broad open arrow corresponds to the free surface

The epoxy resin frequently forms wrinkles on ultrathin sectioning, as can be seen in *Figure 2*, due to the difference in hardness between the sample film and the epoxy resin. The wrinkles appear dark in the micrograph, as shown by the objects marked A, owing to the contrast due to the thickness variation. The wrinkles, however, make it easier to distinguish the epoxy resin from the supporting film and, therefore, the free surface from the other edges of the section. Some other techniques to mark the free surfaces, such as selective staining of the free surfaces, are possible for experts in microtoming. However, it should be noted that there is no guarantee that the ultrathin sections always contain the cross-sectional area of the free surface. There is a large chance that the section edges, which are merely the inner structures of the sample films, can be mistaken for the free surface. Therefore, the marking of the free surfaces by epoxy resin[1] is necessary.

According to our observation, the free surface of HY-12 always consists of a thin layer of PI component stained dark with osmium tetroxide. The same result was also obtained by Ishizu *et al.*[14,15] by a similar technique. This phenomenon was attributed to the thermodynamic requirement to minimize the surface free energy of the block copolymers, i.e. in thermal equilibrium the one having lower critical surface tension should form the outermost layer at a free surface. The average value of critical surface tension reported for PI is certainly smaller than that reported for polystyrene (PS)[1]. Then the question arises whether this is a common phenomenon for different microdomain morphologies or not. This problem is discussed in the next section. It should be noted that the large bright portions marked B in the micrograph may result from swelling of PS microdomains by epoxy during the curing reaction.

Figure 3 shows an electron micrograph of the surface replica of the same cast film of HY-12 representing the surface topology. It is typical of the surface replicas of block copolymers with L_{AB} morphology. A pattern like the cross-grain of wood, which resembles the lamellar microdomain structure observed in the ultrathin section sliced parallel to the surface of a poly(styrene-*b*-butadiene-*b*-styrene) (SBS) block copolymer film[16], can be observed. The narrowest spacing of the striations in the figure (see the portion marked A for example) is similar to that of the lamellar microdomain of HY-12 ($\sim$140 nm measured by small-angle X-ray scattering), and the striations have often been explained as the edges of lamellar microdomains coming out to the free surface. Thus, they generate a small surface undulation associated with the domain structure beneath the surface. However, after close observation of *Figure 2* one will come to the conclusion that this is not always the case. The surface roughness is not always related to lamellar edges. The rough surface may result from the rearrangement of the microdomain structure by the unswelling during the film casting process. Since this structural rearrangement is

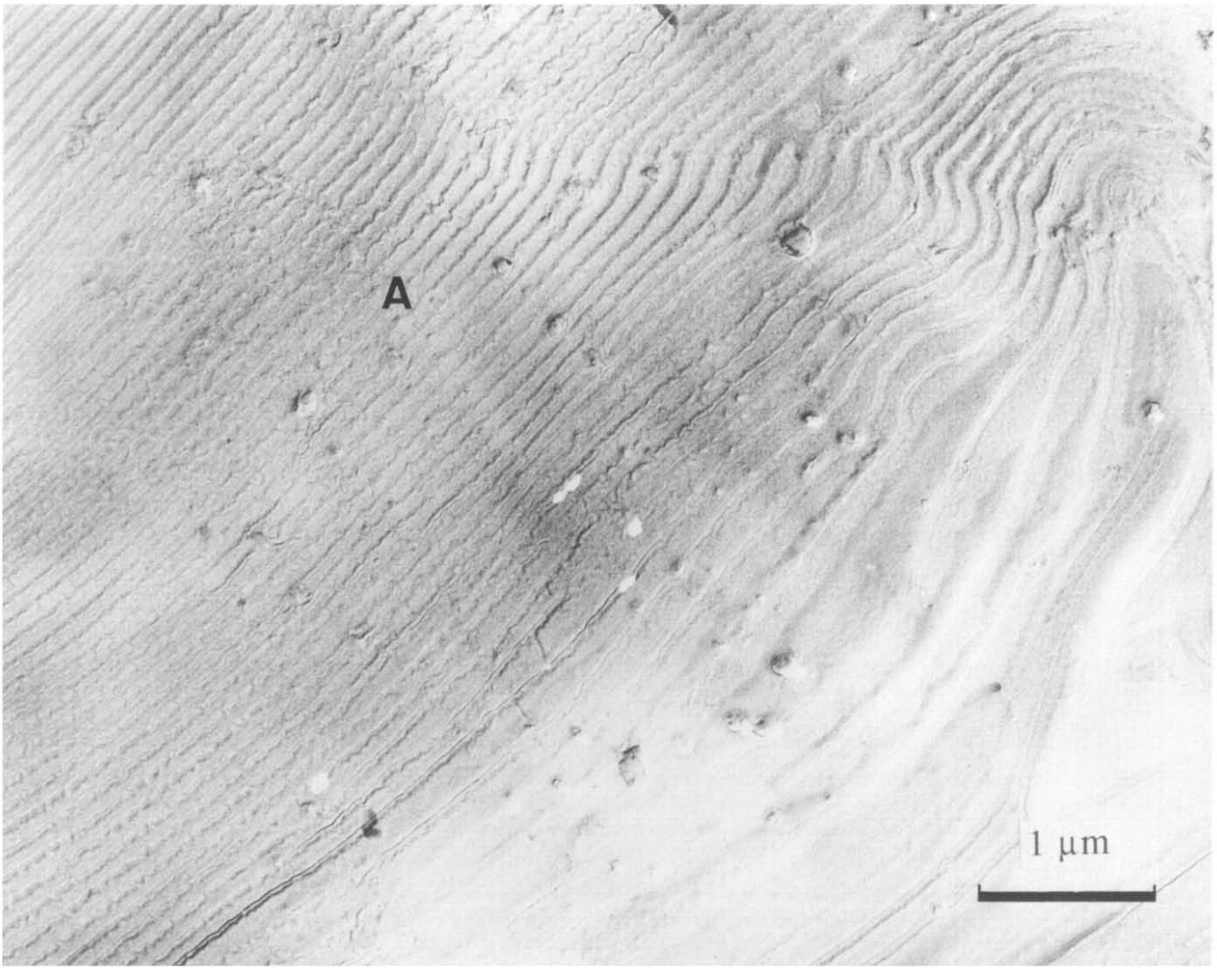

Figure 3 Electron micrograph of the replica of the free surface of HY-12 film cast from toluene solution

related to the orientation of the lamellar microdomain structure, the surface topology is also related to the orientation of the lamellar microdomain structure underneath, resulting in a pattern similar to the parallel section.

Dependence on microdomain morphology

In case of S_{PS} or C_{PS} morphology in which PS forms spherical or cylindrical microdomains in the matrix of PI, it is evidently expected that the outermost layer at the free surface would be composed of PI. This expectation was confirmed with the electron micrograph of an ultrathin section obtained from a toluene-cast film of HK-5 (SI block copolymer with $M_n = 1.82 \times 10^5$ and PS/PI = 31/69 by weight) shown in *Figure 4*, in which the PS component (bright phase) forms cylindrical microdomains dispersed in PI matrix (dark phase). *Figure 4a* shows the region where the cylinder axes are perpendicular to the cross-section, whereas *Figure 4b* shows the region with the cylinder axes more or less in the plane of the cross-section. Resembling the case of lamellar morphology[1,17,18], cylindrical microdomain structures also exhibit a particular orientation: the cylinder axes are aligned parallel to the film surface[19,20]. In particular, the (1 0 0) plane of the hexagonal lattice is parallel to the film surface. However, since the orientation of the cylinder axes within a plane parallel to the film surface is random, both micrographs in *Figures 4a* and *4b* were observed in the same ultrathin section. It is obvious in *Figure 4* that the free surface is covered with a thin layer of PI component. The outermost layer is considered to consist of a monomolecular layer of PI as depicted in Figure 3 of ref. 1. The interstices between the PS cylinders are filled with enough PI to give a flat free surface at the length scale r satisfying $D_C < r < \xi$, where D_C is the intercylinder distance and ξ is the persistence length defined in *Figure 1*. Note that there is a small surface undulation at $r \simeq D_C$ as shown in the sketch inserted in *Figure 4a*.

In the previous paper[1] we reported that the effect of a surface on the internal microdomain is rather small in the case of the L_{SI} morphology except for the effect on the microdomain orientation. Surface-induced microphase separation and microdomain orientation were reported by some workers[3,14,15,21–23]. The following speculation provides some possibility that a significant surface effect other than these two might exist for spherical and cylindrical microdomain morphologies. The cross-sections of PS cylinders in *Figure 4a* exhibit oval but not circular shapes, oval shapes with their long axes perpendicular to the free surface (i.e. along the *Oz*

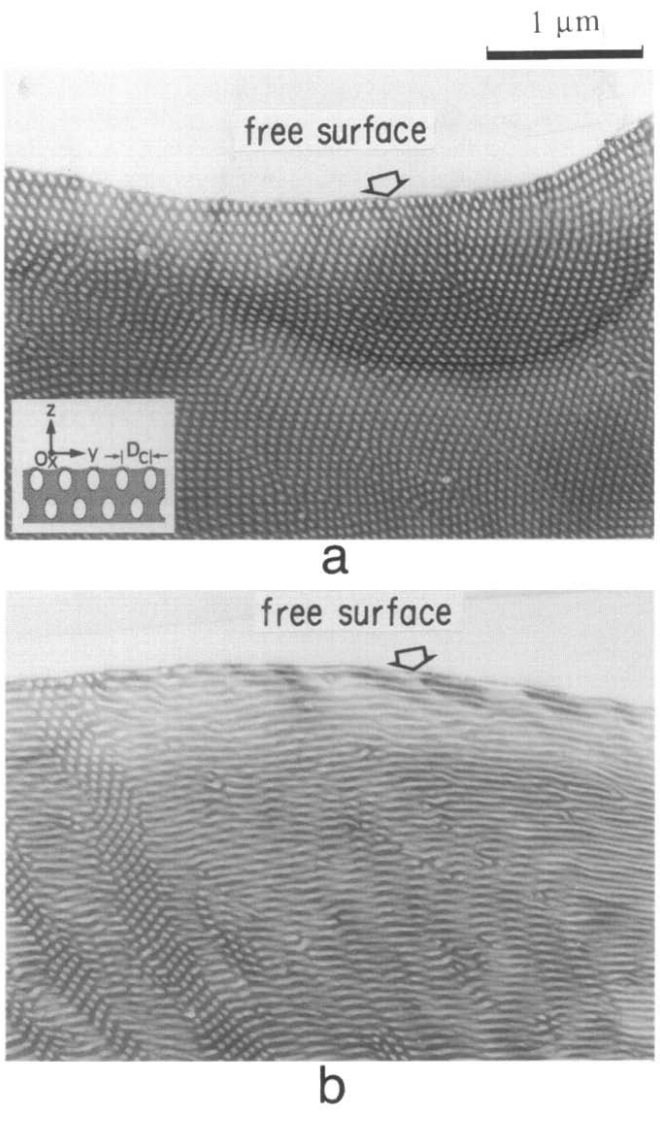

Figure 4 Electron micrographs of ultrathin sections of HK-5 (SI) film cast from toluene solution: (a) the region where the cylinder axes are perpendicular to the cross-section; (b) the region where the cylinder axes are more or less in the plane of the cross-section

axis). The shapes cannot be attributed to either the tilting of the cylinder axes or the deformation of cylinders driven by the stress exerted on the films during the solvent evaporation process. The tilting of cylinder axes away from the Ox direction by a rotation around the Oy axis in the plane of Oxz may generate the oval shape observed. However, such tilting is obviously prohibited. If the tilting occurs, it should tilt the cylinder axes around the Oz axis in the plane of Oxy, giving rise to oval cross-sections with their long axes oriented in the opposite direction, i.e. parallel to the Oy axis. Thus, tilting is not the case. The stress exerted on the film is expected to give rise to the oval-shaped cross-section oriented again in the opposite direction[24]. This is because the film can shrink freely in the thickness direction (Oz axis) but cannot do so in the directions normal to the Oz axis; the dimensions of the films in the Oxy plane are essentially fixed and constrained to the surface of the Petri dishes. The constraint gives rise to a tension in the film and hence to the deformation of the cylinders such that their cross-sections are oval with their long axes oriented along the Oy axis. This deformation was actually observed by SAXS (see Figure 19 of ref. 19 and Figures 6 and 9 of ref. 24) and will be reported elsewhere[20]. Thus, this deformation cannot account for the experimental results. The oval-shaped cross-sections may be best understood in terms of deformation driven by a 'surface effect', viz. with this deformation the PI block chains tend to come closer to the surface while the PS block chains tend to go away from the surface.

In the case of C_{PI} and S_{PI} in which PI component forms cylindrical and spherical microdomains, respectively, dispersed in PS matrix, it is not obvious whether the PI component can form the outermost layer at a free surface or not. Since curved interfaces are thermodynamically preferred for such systems, flat free surfaces with PI components as the outermost layer may not be the best way to minimize the net free energy.

Figure 5a shows an electron micrograph of the cross-section of the free surface of the toluene-cast film of HS-11 (SI block copolymer with $M_n = 8.50 \times 10^5$ and PS/PI = 80/20 by weight), which exhibits a typical S_{PI} morphology. The micrograph reveals that the free surface is again totally covered with a very thin layer of PI, the thickness of which appears to be smaller than half of the average PI domain size or the radius of the PI spherical microdomains ($R_{PI,S}$). This is in contrast to the case of

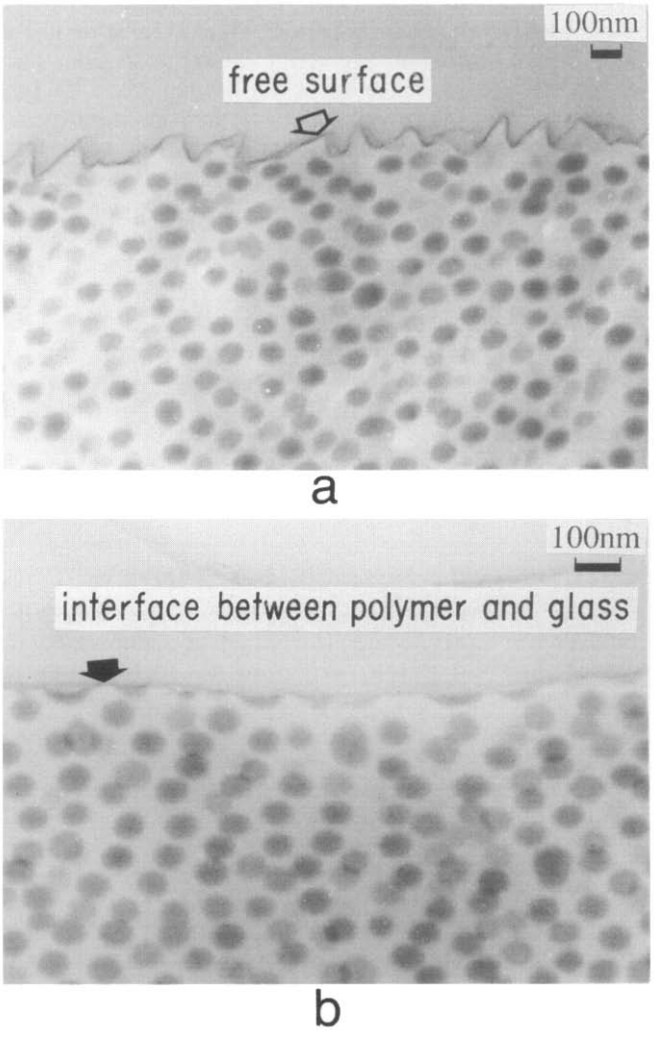

Figure 5 Electron micrographs of ultrathin sections of HS-11 (SI) film cast from toluene solution: (a) cross-section near the free surface; (b) cross-section near the interface between the polymer and the glass substrate (Petri dish)

L_{SI} morphology. The thickness of the surface PI layer (d_L) of L_{SI} is about half of the thickness of the average PI lamellar microdomain (D_{PI}) in the bulk:

$$d_L \simeq \tfrac{1}{2}D_{PI} \quad (1)$$

This result in the L_{SI} case suggests that the number of block copolymer chains per unit interfacial area (N_c) for the outermost layer (monomolecular layer, see Figure 3 of ref. 1) is the same as that for the inner lamella (bimolecular layer). If this criterion also holds for the C_{PI} and S_{PI} morphologies, the thickness of the surface PI layer (d_C and d_S) becomes one-half of the radius of the PI cylinders ($R_{PI,C}$) and one-third of the radius of the PI spheres, respectively:

$$d_C = \tfrac{1}{2}R_{PI,C} \quad \text{(for } C_{PI}\text{)} \quad (2)$$

$$d_S = \tfrac{1}{3}R_{PI,S} \quad \text{(for } S_{PI}\text{)} \quad (3)$$

Evaluation of d_S and $R_{PI,S}$ of HS-11 from the electron micrographs is not straightforward. Since the thickness of the ultrathin section is about 50 nm and the diameter of the PI spherical microdomain is larger than 50 nm, many of the observed PI microdomains are projections of only small portions of spherical microdomains. Such microdomains that appear brighter and smaller than the others and should be omitted from the evaluation. The average radius of the PI spherical microdomains thus evaluated is ~40 nm. Similarly, the projection of the PI surface layer may appear wider than it is, if it is not normal to the surface of the ultrathin section. This is because the surface layer is thinner than 50 nm. Therefore, d_S was evaluated from the thickness of the surface layer with the appearance of clear edges, and the average value was ~13 nm, which was about one-third of $R_{PI,S}$. This suggests that N_c for the outermost layer at the free surface is similar to that of the microdomains inside the film. It should be emphasized, however, that this criterion on the thickness of the free surface layer is only a crude estimation and applicable only to the morphologies with PS matrix. It is interesting and a surprise to note that N_c for the interface between PS and PI in the free surface (denoted as $(N_c)_{free}$) is the same as that in the bulk (denoted as $(N_c)_{obs}$), despite the fact that the PI block chains in the former contact with air and those in the latter contact with the PI block chains themselves:

$$(N_c)_{free} \simeq (N_c)_{obs} \quad \text{(for any morphologies)} \quad (4)$$

For the solvent-cast films of SI block copolymers, the observed $R_{PI,S}$ ($(R_{PI,S})_{obs}$) is much smaller than its equilibrium value[25] ($(R_{PI,S})_{eq}$). The $R_{PI,S}$ value is related to N_c by:

$$R_{PI,S} = 3N_c v_{c,PI} \quad (5)$$

where $v_{c,PI}$ is the volume occupied per single PI block chain. Thus, the fact that $(R_{PI,S})_{obs} < (R_{PI,S})_{eq}$ suggests that:

$$(N_c)_{obs} < (N_c)_{eq} \quad (6)$$

where $(N_c)_{eq}$ is the equilibrium value of N_c for the domains in the bulk. Equation (6) together with equation (4) leads us to conclude that N_c for the layer in the free surface ($(N_c)_{free}$) is smaller than $(N_c)_{eq}$ in the bulk, i.e.:

$$(N_c)_{eq} > (N_c)_{free} \quad \text{(for PI spherical microdomains)} \quad (7)$$

There remain the following questions: (i) Is the value $(N_c)_{free}$ ($4.4 \times 10^{-4}\,nm^{-2}$) thus estimated using the relationship of equations (4) and (5) and $R_{PI,S} = (R_{PI,S})_{obs}$ the equilibrium one or not? (ii) Is the observation of the relation of equations (4) or (3) merely accidental or not, and how does d_S change with the film preparation conditions, e.g. the rate of solvent evaporation? Answering these questions deserves future investigations.

When the discussion given above is applied to the C_A, C_B and L_{AB} morphologies, one obtains the following conclusions:

$$(N_c)_{eq} \simeq (N_c)_{free} \quad \text{(for lamellar and PI cylindrical microdomains)} \quad (8)$$

It should be noted here that

$$\tfrac{1}{2}D_{PI} = N_c v_{c,PI} \quad (9)$$

$$R_{PI,C} = 2N_c v_{c,PI} \quad (10)$$

and that the observed D_{PI} and $R_{PI,C}$ can be close to the corresponding equilibrium values[13], giving rise to:

$$(N_c)_{obs} \simeq (N_c)_{eq} \quad \text{(for lamellar and PI cylindrical microdomains)} \quad (11)$$

Figure 5b shows a cross-section of the interface between the same block copolymer (HS-11) and the glass (the Petri dish). In this case we are not as confident about the results as in the case of the free surface because the real interfacial layer might be stuck on the glass surface and peeled off from the film specimen. Since the critical surface tension of the glass is considered to be much larger than that of PS, it is likely that the PS component comes to the interface and forms a similar interfacial layer to the PI surface layer observed in *Figure 4*. Nevertheless, the interfacial layer seen in *Figure 5b* again consists of the PI component. However, this does not mean that the interfacial layer has been peeled off. The electron micrograph seems to reveal the real interface because the morphology of the outermost phase consisting of PI is quite different from the internal structure. The outermost PI phase has a shape like an array of concave lenses, the diameter of which is much larger than that of the inner PI spherical microdomains. The lens-shaped PI microdomains are connected to each other by a thin layer of PI, so that the whole interfacial area is covered with the PI component. We would rather consider that the glass surface must have been covered with an oily impurity that reduced the surface free energy and that the PI component is in contact with this impurity.

It should be noted that the roughness of the free surface in *Figure 5a* and that of the interface in *Figure 5b* are quite different. The interface between the glass and the polymer is much smoother than the free surface, as expected. *Figure 5a* reveals that the topology of the rough free surface bears no relation to the inner structure of the PI spherical microdomains. On the other hand, the topology of the interface with the glass is directly related to the shape of the interfacial PI phases. This difference can be observed more directly in the two-stage replicas of the free surface and the interface in *Figure 6*, in which concave parts of the sample film appear convex and its convex parts appear concave. *Figure 6b* shows the replica of the interface, and each circular protuberance corresponds to one of the concave-lens-shaped PI microdomains, whereas *Figure 6a*, the replica of the free surface, exhibits a peculiar pattern, i.e. the area is divided into cells of different sizes containing one or more

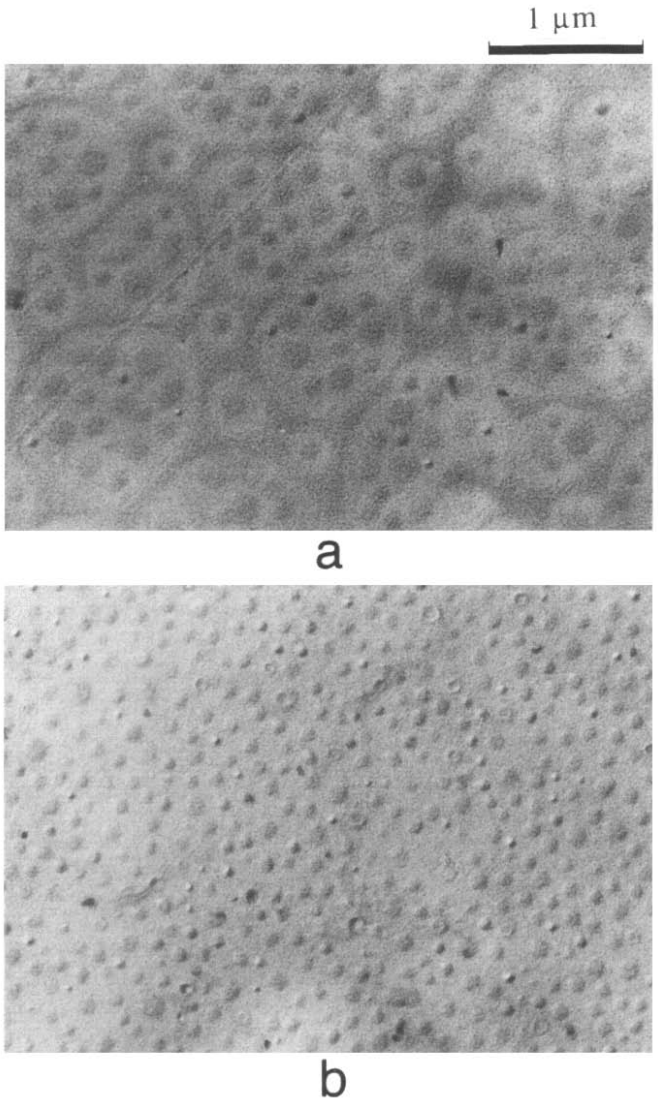

Figure 6 Electron micrographs of the replica of HS-11 film cast from toluene solution: (a) free surface; (b) surface on the glass substrate (Petri dish) side of the cast film

protuberances of nearly uniform size that correspond to the lateral dimension of the surface roughness (concave regions) in *Figure 5a*. Note that the size is about three times as big as the diameters of the PI spherical domains. The origin of such a pattern is not known, but it may result from the stress exerted on the films during unswelling and reorganization of the packing of the PI microdomains in the film casting process.

Dependence on casting solvent

It is well known that the microdomain morphology of block copolymer films cast from solutions depends on the casting solvent[8,10]. *Figure 7* shows the effect of the casting solvent on the microdomain and free surface morphology of the same SI block copolymer, HY-10 ($M_n = 1.64 \times 10^5$ and PS/PI = 69/31 by weight). HY-10 is supposed to have a T_{PI} (PI tetrapod network in PS matrix) morphology in its bulk equilibrium state as observed in its toluene-cast film (*Figure 7b*)[8]. Since cyclohexane is a selectively good solvent for the PI component, the microdomain morphology changes to L_{SI} (*Figure 7a*). When selective solvents for the PS component were used, the microdomain morphology changes to C_{PI} (*Figure 7c* for styrene monomer) or to S_{PI} (*Figure 7d* for 1,4-dioxane) depending on the *affinity* of the solvent. Regardless of the casting solvent or the microdomain morphology, the free surface of the cast films is always covered with thin (monomolecular) layers of the PI component.

The outermost PI layer of the L_{SI} morphology (*Figure 7a*) is relatively smooth and flat in contrast to the toluene-cast film of HY-12 (*Figure 2*). This may be attributed to the size of the grains, which affects the reorganization process of the microdomains during solvent evaporation[13]. According to our observations, the smaller the molecular weight, the smoother the free surface on a microscopic scale in the observed molecular-weight range of 3×10^4 to 1×10^6. In general, the size of the grains is larger for small-molecular-weight block copolymers than for large-molecular-weight ones.

In the case of the T_{PI} structure (*Figure 7b*), the outermost PI layer is relatively smooth and underneath it is a PS layer, which disturbs the connectivity between the outermost layer and the PI network. Such a surface morphology should affect certain properties of the block copolymer membrane, such as the gas permeability[26], even if it has the bicontinuous microdomain morphology in the bulk.

The roughness of the free surface increases as the PI component forms dispersed microdomains. An extremely rough surface was observed again for the S_{PI} morphology (*Figure 7d*) as in the case of HS-11 (*Figure 5a*).

The thickness of the PI surface layer for the L_{SI} morphology (d_L) is 12 ± 2 nm and about half of the thickness of the inner PI lamellar microdomains ($D_{PI} = 23.1$ nm)[8]. The thickness of the PI surface layer for the T_{PI} morphology (d_T) is also about 12 nm. For the C_{PI} morphology d_C is 12 ± 2 nm and about half of the radius of the PI cylinders ($R_{PI} = 18.9$ nm by small-angle X-ray scattering (SAXS) analysis and $R_{PI} = 22 \pm 2$ nm by electron microscopy (EM))[8]. However, the thickness of the PI surface layer (d_S) becomes significantly thinner for the S_{PI} morphology, and is 6 ± 3 nm, about one-third of the radius of the inner PI spherical microdomains ($R_{PI} = 15.2$ nm by SAXS analysis and $R_{PI} = 17 \pm 2$ nm by EM)[8]. These results are in good agreement with the criterion of identical N_c for the surface layer and the internal microdomains discussed in the previous section (equation (4)) although it must be admitted that the thickness of the surface layer varies with the internal microdomain structure even when the same block copolymer is used. The same results are obtained for the L_{SI}, T_{PI} and C_{PI} morphologies:

$$d_L \simeq d_T \simeq d_C \simeq 12 \text{ nm} \qquad (12)$$

suggesting that N_c in the bulk or $(N_c)_{free}$ is almost the same for the three morphologies. Only the S_{PI} morphology has a significantly smaller value for d_S and hence for $(N_c)_{free}$, suggesting that non-equilibrium may affect not only the microdomain structure but also the surface structure.

The above results together with the results discussed in conjunction with equation (4) imply the following point. Both $(N_c)_{obs}$ and $(N_c)_{free}$ increase with increasing segregation power invoked by increased polymer concentration during solvent evaporation. However, once the non-equilibrium effects[13] become serious, and the domain size in the bulk or $(N_c)_{obs}$ is frozen-in, the domain sizes (d_{PI}) or $(N_c)_{free}$ at the free surface may also be frozen-in,

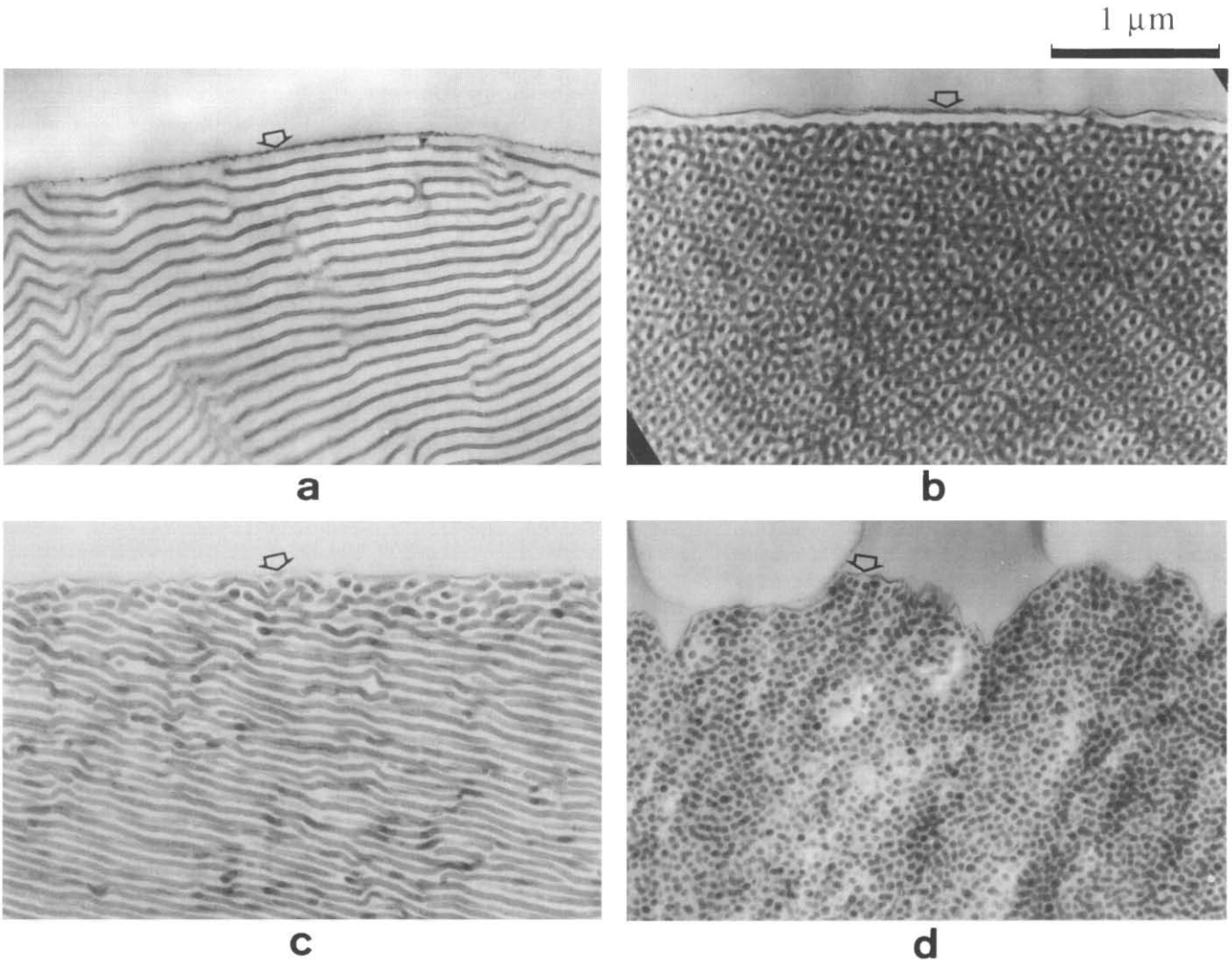

Figure 7 Electron micrographs of ultrathin sections near the free surface of HY-10 films cast with various solvents: (a) cyclohexane; (b) toluene; (c) styrene (monomer); (d) 1,4-dioxane

resulting in equation (7) for the S_{PI} morphology. For the other morphologies such as L_{SI}, T_{PI} and C_{PI} equation (8) is applied.

Effect of annealing above the glass transition temperature

The non-equilibrium surface morphology was intentionally made by fracturing HY-12 toluene-cast film. The fractured surface was prepared perpendicular to the film surface. Since most of the lamellae have an orientation with their interfaces parallel to the film surface, most of the lamellar interfaces are found to be perpendicular to the fractured surface under microscopic observation. Throughout the entire processes[1] of preparing the ultrathin sections containing the cross-sectional views of the fractured surface, the PS phases are kept in the glassy state to avoid structural rearrangement as much as possible. Under this condition, both PI and PS components are observed to be exposed at the fractured surface, though such a surface structure is unfavourable because it has a higher surface free energy than that covered with the PI component alone.

Figure 8 shows the fractured surface after annealing at ~150°C for 1 min and quenching into ice-water. The whole area of the fractured surface is clearly seen to have changed into the morphology entirely covered with the PI component. Annealing above the glass transition temperature of PS even for such a short time is found to be sufficient to allow molecular rearrangement leading to the equilibrium structure. This rearrangement must be a considerably fast process. The observation of this process itself by electron microscopy may be an interesting future work.

Effect of crystalline component

The morphology of amorphous–crystalline block copolymers has been investigated by several groups[2,27–31], but it is not so well understood as that of amorphous–amorphous block copolymers. The morphology is more complicated for block copolymers containing crystalline components than those without because the former involves two kinds of phase transitions, namely microphase separation and crystallization, while the latter involves only microphase separation. Therefore, the morphology of the free surfaces of amorphous–crystalline block copolymers is also expected to be more complicated than that of amorphous–amorphous block copolymers. Since crystallization is a non-equilibrium process, both bulk and surface morphologies of an amorphous–crystalline block copolymer must be significantly affected by the crystallization of one component as well as by

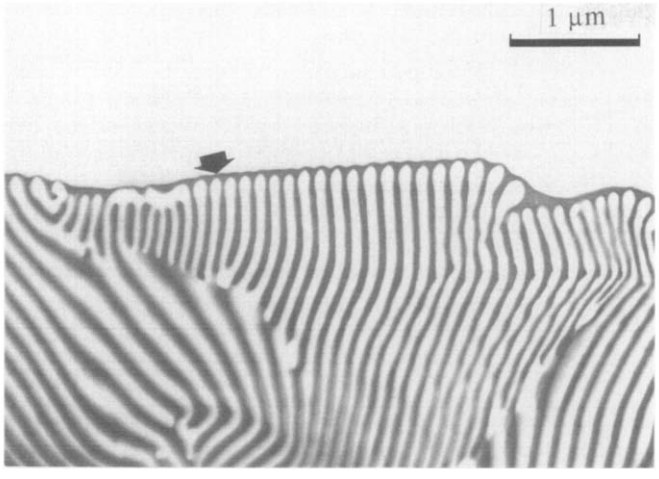

Figure 8 Electron micrograph of ultrathin section of the fractured surface of HY-12 film cast from toluene solution and annealed at ~150°C for ~1 min

whether crystallization or microphase separation occurs first[29,31].

Figure 9 shows a surface replica of a film of a multiblock copolymer of nylon-6,10 and PPO (61P3-56)[6,7] cast from *m*-cresol solution. Since nylon-6,10 is crystallizable, volume-filling spherulites of several micrometres in diameter are observed in *Figure 9a* obtained for the two-stage replica. A higher-magnification micrograph (*Figure 9b*) reveals the edges of the spherulite exposed to the free surface.

Figure 10 shows ultrathin sections of 61P3-56 exhibiting the cross-section near the free surface. The specimen was stained with ruthenium tetroxide (RuO_4), which is known to stain nylons or poly(ethylene oxide-*co*-propylene oxide)[32]. But the staining result for PPO homopolymer is not reported. The low-magnification micrograph (*Figure 10a*) shows close-packed spherulites stained dark with RuO_4, which is consistent with the observation in the surface replica. The free surface of the cast film with an array of the spherulites. In addition, *Figure 10a* shows the unstained interstices between the spherulites. We consider that these interstices are composed of PPO homopolymer mixed with the block copolymer during synthesis. It suggests that PPO homopolymer is not stained by RuO_4. However, the staining behaviour of RuO_4 has not been clearly understood, and interpretation of the electron micrographs is not so straightforward as in the case of staining with osmium tetroxide. When RuO_4 is applied to SI block copolymers, we often observe the effect that the interfacial area is most extensively stained. In the case of crystalline homopolymers such as polyethylene, polypropylene and nylons, we observed that amorphous regions are extensively stained. *Figure 10b* shows the high-magnification micrograph of the cross-section of one of the spherulites at the free surface. Judging from our experience we consider that the unstained regions in *Figure 10b* correspond to the crystalline lamellae of the nylon-6,10 component of 61P3-56 and the stained regions to the PPO component and some amorphous nylon-6,10. Admitting this designation, *Figure 10b* exhibits the phase-separated structure of 61P3-56 that results from the crystallization of nylon-6,10 rather than the microphase separation between nylon-6,10 and PPO. The free surface is also affected by this process of structure formation. The composition of the free surface depends on the orientation of the crystalline lamellae. When the crystalline lamellae are parallel to the free surface, the amorphous PPO layer is exposed to the free surface. (The outermost layer is stained dark.) On the other hand, when the edges of the crystalline lamellae come out to the surface, both components can be exposed to the free surface and form a multicomponent free surface. (Alternating stained and unstained regions are observed.) This situation is schematically illustrated in *Figure 11*. This phenomenon has been observed for other amorphous–crystalline block copolymers[2,30], and a similar model has been proposed by Thomas and O'Malley[2]. Presumably the models sketched in *Figure 11* are reasonable morphology when crystallization occurs prior to microphase separation during the solvent evaporation process. When microphase separation occurs prior to crystallization, there may be a possibility that the component having lower surface tension covers the free surface even in the case when crystallization takes place.

Mixture of two block copolymers

Figure 12 shows an electron micrograph of a 50/50 wt% mixture of HY-12 (SI block copolymer) and TOKI-12 (SB block copolymer, $M_n = 9.99 \times 10^4$ and PS/PI = 52/48 by weight) cast from toluene solution. HY-12

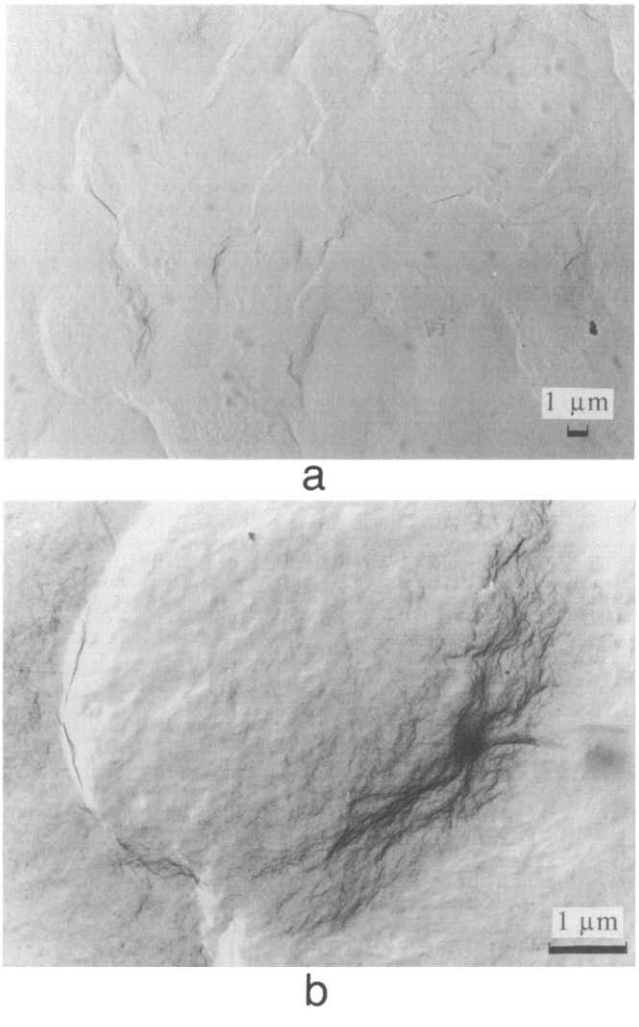

Figure 9 Electron micrographs of the replica of the free surface of the nylon-6,10–poly(propylene oxide) multiblock copolymer (61P3-56) film cast from *m*-cresol solution: (a) low magnification; (b) high magnification

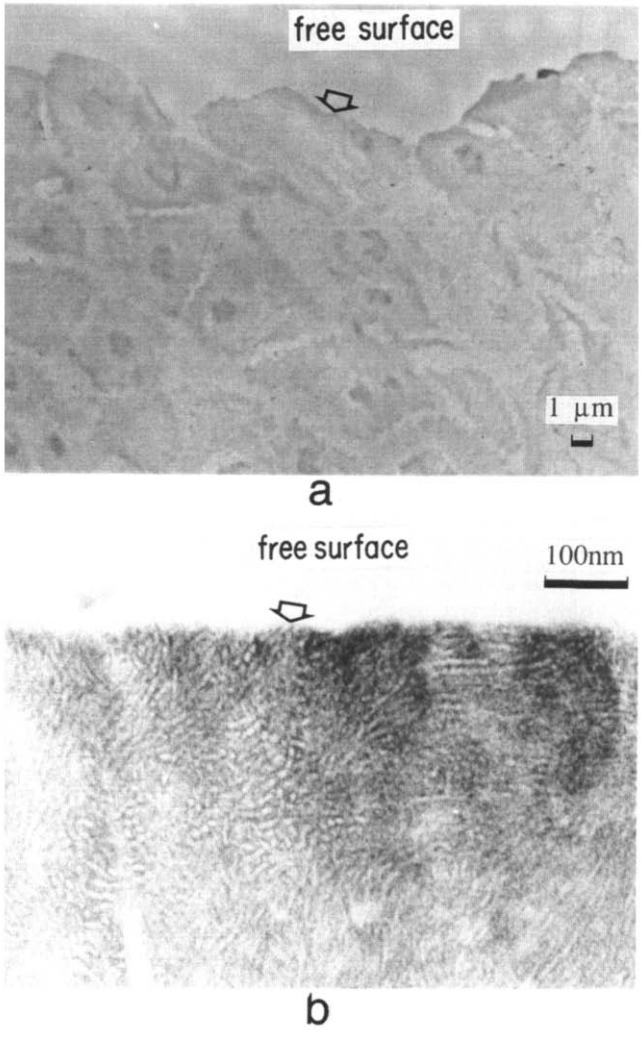

Figure 10 Electron micrographs of ultrathin sections near the free surface of the 61P3-56 film cast from *m*-cresol solution and stained with ruthenium tetroxide: (a) low magnification (closely packed spherulites); (b) high magnification (inside of one of the spherulites at the free surface)

was synthesized in THF, a polar solvent, and the microstructure of the PI component is rich in vinyl (3,4-) linkages[33]. On the other hand, TOKI-12 was synthesized in benzene, a non-polar solvent, and the microstructure of the PB component is rich in 1,4-linkages. Although these two block copolymers have the PS component in common, they underwent macroscopic phase separation because 3,4-polyisoprene and 1,4-polybutadiene are highly immiscible[34,35]. It is conceivable that the difference in molecular weight may also be a reason for the phase separation[36]. Consequently two kinds of lamellar microdomain structures were observed in the cast film. Owing to the difference in microstructure, which affects the efficiency of staining with osmium tetroxide, and to the large difference in microdomain spacing that results from the difference of about five times in molecular weight, it is quite easy to distinguish the SI microdomains (the lamellae with the larger spacing) from the SB microdomains (the lamellae with the smaller spacing and darker PB phase) in the electron micrograph. The regions rich in SB block copolymers are marked by SB with white broken border lines in *Figures 12* and *13*. It was found that the free surface was preferentially covered with polybutadiene layers, and, therefore, by the SB block copolymer. It appears that there is some discontinuity of the outermost PB layer in the region in which the SB lamellae, L_{SB}, have orientation more or less perpendicular to the free surface (the portions marked by X in the micrograph), i.e. the PS phase of the SB block copolymer is exposed to the free surface as well as the PB phase. A similar surface morphology is frequently observed also for the cast film of neat TOKI-12, again when the lamellae emerge perpendicular to the free surface. The reported values of the critical surface tension for PB[37] are 31 mN m^{-1} for 1,4-*trans*, 32 mN m^{-1} for 1,4-*cis* and 25 mN m^{-1} for 1,2- (vinyl), and that for PS[38] is typically 30–33 mN m^{-1}, very close to the values for 1,4-microstructure of PB. This may be the reason why both PB and PS components can be exposed to the free surface. However, PB has a statistically higher tendency to be spread along the free surface than PS. Note that the change in the thickness of the dark lamellae at the locations marked by A is due to the change of orientation of the PI lamellae in SI.

It should be emphasized that the free surface always consists of the SB block copolymer but not the SI block copolymer. It was even observed that a single (monomolecular) layer of the SB block copolymer is covering the surface as shown in the portion marked by Y in *Figure 12*. Such a portion is more clearly observed in *Figure 13*. *Figure 13* shows the free surface for the same block copolymer as in *Figure 12*. The portion Y of the free surface between the two small SB grains at the surface (marked by SB) corresponds to the monomolecular layer of the SB block copolymer that directly contacts with L_{SI} (marked by SI). In contrast to the surface of L_{SB} multilamellar layers shown in the portion X in *Figure 12*, this surface Y is continuously covered by the SB monomolecular layer, without a discontinuity or break. In this case, the SB layer was seen as if it had been supplied from the reservoir (SB) of the large stack of SB lamellae adjacent to that area. The reported values of the critical surface tension for PI[38] are 30–31 mN m^{-1} for 1,4-*trans* and 31–32 mN m^{-1} for 1,4-*cis*, but the value for vinyl is not reported. Since the critical tension for vinyl is smaller than that for 1,4- in the case of PB, the same tendency is expected for PI. Therefore, the PI of HY-12, which is rich in 3,4-linkages (vinyl linkages), should have a smaller critical surface tension than the

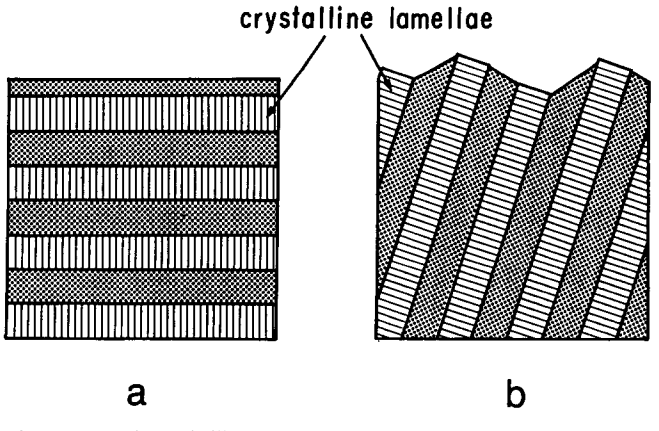

Figure 11 Schematic illustration of the free surface morphology of an amorphous–crystalline block copolymer film. (a) Crystalline lamellae are parallel to the surface: the free surface is covered with the amorphous component. (b) Crystalline lamellae are not parallel to the surface: both crystalline and amorphous components are exposed to the surface

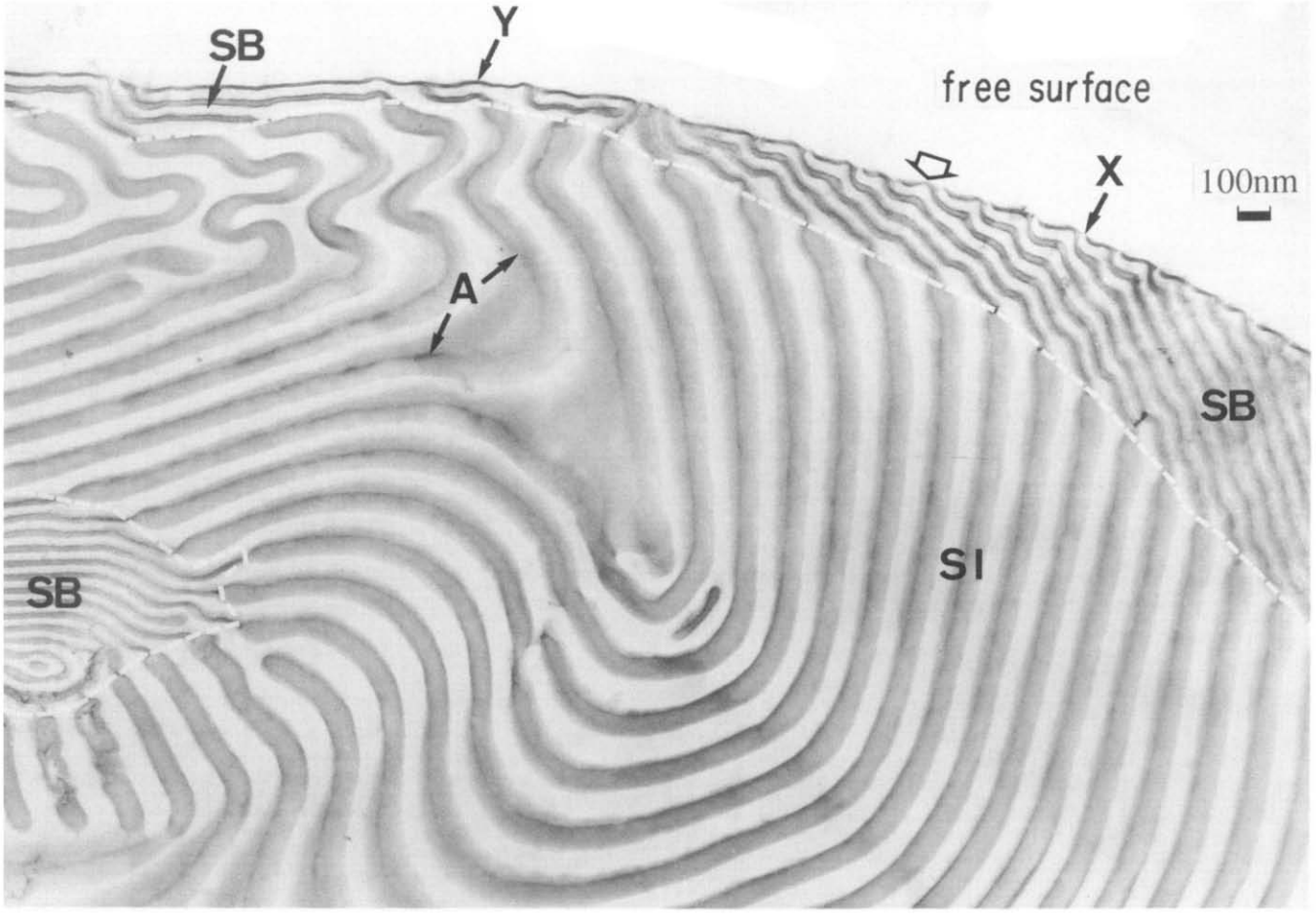

Figure 12 Electron micrograph of the ultrathin section near the free surface of the 50/50 wt% mixture of HY-12 (SI, large molecular weight) and TOKI-12 (SB, small molecular weight) film cast from toluene solution. PB is stained darker with osmium tetroxide than PI

PB of TOKI-12, which is rich in 1,4-linkages according to the reported results[33].

In view of the previous reports on surface tension, our results predict an opposite tendency, the surface tension increasing in the order of 1,4-PB, 3,4-PI and PS. This discrepancy offers an interesting puzzle, the investigation of which deserves future research. Early reports should be rechecked in terms of dependences of surface tension on microstructure and molecular weight. The connectivity between PS and PI block chains in SI or between PS and PB block chains in SB may also have to be considered in predicting the surface morphology. We would like to emphasize here that our technique is quite sensitive to a subtle difference in the surface tension of the constituent polymers. Our technique can be applied also to polymer blends in general.

CONCLUSIONS

The free surfaces of block copolymers consisting of amorphous components obey the thermodynamic requirements, i.e. the constituent block chains with lower critical surface tension cover the free surface. This phenomenon was observed even for block copolymer films in which the component with lower critical surface tension forms the dispersed phases (spheres or cylinders) and the component with higher critical surface tension forms the matrix. The casting solvent has no effect on this behaviour except for the effect on the internal microdomain morphology. The thickness of the outermost layer at the free surfaces can be estimated by assuming a constant number density of block copolymer chains at microdomain interfaces for morphologies having the higher critical surface tension component as the matrix. Under this criterion equation (4) was found experimentally, which further predicts equation (7) for spherical microdomains and equation (8) for lamellar, tetrapod and cylindrical morphologies.

On the other hand, the free surfaces of block copolymers with crystalline components are governed by the crystallization kinetics and the priority of crystallization and microphase separation during the solvent evaporation process. Especially in the case when crystallization occurs prior to microphase separation, the surface morphology and surface composition depend on the orientation of the crystalline lamellae at or near the free surface. Therefore, the surface composition may vary with the preparation methods of the films. Both amorphous and crystalline components can be exposed to the free surface if the lamellae edges come out to the surface.

For a cast film of a mixture of SI and SB block copolymers, the free surface is preferentially covered with SB block copolymers. The reason why SB is preferred to PI at the free surface is not clear in view of the reported results of the critical surface tension of PS, PB and PI. Clearly our observations (in *Figures 12* and *13*) suggest

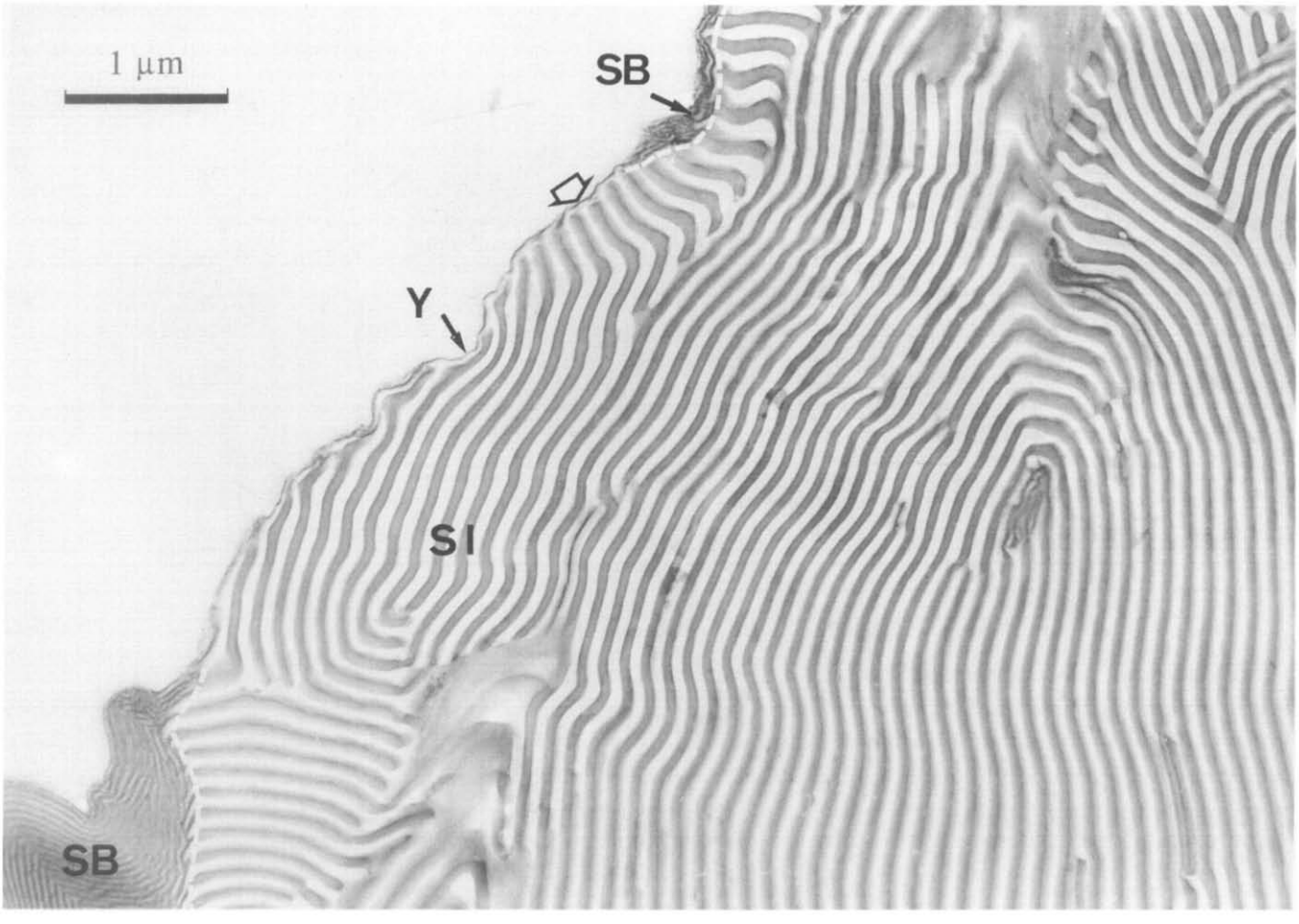

Figure 13 The same ultrathin section as *Figure 12* but different area. A single monomolecular layer of TOKI-12 is seen to be supplied from the large stack of TOKI-12 lamellae

that the surface tension should increase in the order of PB, PI and PS. Finally our technique is claimed to be very sensitive to a subtle difference in the surface tensions of the constituent polymers and to be applicable to polymer blends in general.

ACKNOWLEDGEMENTS

The authors are grateful to Professors K. Sanui and N. Ogata, Sophia University, Tokyo, Japan, for providing the polymer sample 61P3-56 and the late Professor T. Fujimoto at Nagaoka University of Technology, Niigata, Japan, for helping them to synthesize the polymer sample TOKI-12. Part of this work was supported by a Grant-in-Aid for Scientific Research from The Ministry of Education, Science and Culture, Japan (00540009).

REFERENCES

1 Hasegawa, H. and Hashimoto, T. *Macromolecules* 1985, **18**, 589 and references therein
2 Thomas, H. R. and O'Malley, J. J. *Macromolecules* 1979, **12**, 323
3 Fredrickson, G. H. *Macromolecules* 1987, **20**, 2535
4 Patel, N. M., Dwight, D. W., Hedrick, J. L., Webster, D. C. and McGrath, J. E. *Macromolecules* 1988, **21**, 2689
5 Green, P. F., Christensen, T. M., Russell, T. P. and Jerome, R. *Macromolecules* 1989, **22**, 2189; *J. Chem. Phys.* 1990, **92**, 1478
6 Yui, N., Tanaka, J., Sanui, K. and Ogata, N. *Makromol. Chem.* 1984, **185**, 2259
7 Yui, N., Tanaka, J., Sanui, K., Ogata, N., Kataoka, K., Okano, T. and Sakurai, Y. *Polym. J.* 1984, **16**, 119
8 Hasegawa, H., Tanaka, H., Yamasaki, K. and Hashimoto, T. *Macromolecules* 1987, **20**, 1651
9 Hashimoto, T., Koizumi, S., Hasegawa, H., Izumitani, T. and Hyde, S. T. *Macromolecules* in press
10 Inoue, T., Soen, T., Hashimoto, T. and Kawai, H. *J. Polym. Sci. (A-2)* 1969, **7**, 1283
11 Thomas, E. L., Alward, D. B., Kinning, D. J., Martin, D. C., Handlin, Jr, D. L. and Fetters, L. J. *Macromolecules* 1986, **19**, 2197
12 Krigbaum, W. R., Yazgan, S. and Tolbert, W. R. *J. Polym. Sci., Polym. Phys. Edn.* 1973, **11**, 511
13 Mori, K., Hasegawa, H. and Hasimoto, T. *Polymer* 1990, **31**, 2368
14 Ishizu, K. and Fukuyama, T. *Macromolecules* 1989, **22**, 244
15 Ishizu, K., Yamada, Y. and Fukutomi, T. *Polymer* 1990, **31**, 2047
16 Matsuo, M., Ueno, T., Horino, S., Chujyo, S. and Asai, H. *Polymer* 1968, **9**, 425; Matsuo, M. *Jap. Plast.* 1968, **2**, 6
17 Hashimoto, T., Todo, A., Itoi, H. and Kawai, H. *Macromolecules* 1977, **10**, 377
18 Hashimoto, T., Shibayama, M. and Kawai, H. *Macromolecules* 1980, **13**, 1237
19 Hashimoto, T., Shibayama, M., Fujimura, M. and Kawai, H. in 'Block Copolymer Science and Technology', (Ed. D. J. Meier), MMI Press, Harwood Academic, New York, 1983, p. 63
20 Mori, K., Hasegawa, H. and Hashimoto, T. in preparation
21 Henkee, C. S., Thomas, E. L. and Fetters, L. J. *J. Mater. Sci.* 1988, **23**, 1685

22 Coulon, G., Russel, T. P., Deline, V. R. and Green, P. F. *Macromolecules* 1989, **22**, 2581
23 Russel, T. P., Coulon, G., Deline, V. R. and Miller, D. C. *Macromolecules* 1989, **22**, 4600
24 Todo, A., Uno, H., Miyoshi, K., Hashimoto, T. and Kawai, H. *Polym. Eng. Sci.* 1977, **17**, 587
25 Hashimoto, T., Fujimura, M. and Kawai, H. *Macromolecules* 1980, **13**, 1660
26 Kinning, D. J., Thomas, E. L. and Ottino, J. M. *Macromolecules* 1987, **20**, 1129
27 Lotz, B. and Kovacs, A. J. *Kolloid-Z. Z. Polym.* 1966, **209**, 97; Lotz, B., Kovacs, A. J., Bassett, G. A. and Keller, A. *Kolloid-Z Z. Polym.* 1966, **209**, 115
28 Kawai, T., Shiozaki, S., Sonoda, S., Nakagawa, H., Matsumoto, T. and Maeda, H. *Makromol. Chem.* 1969, **128**, 252
29 Hirata, E., Ijitsu, T., Soen, T., Hashimoto, T. and Kawai, H. *Polymer* 1975, **16**, 249
30 Takahashi, A. and Yamashita, Y. in 'Copolymers, Polyblends and Composites', (Ed. A. J. Platzer), American Chemical Society, Washington, DC, 1975, p. 267
31 Cohen, R. E., Cheng, P.-L., Douzinas, K., Kofinas, P. and Verney, C. V. *Macromolecules* 1990, **23**, 234
32 Trent, J. S., Scheinbeim, J. I. and Couchman, P. R. *Macromolecules* 1983, **16**, 589
33 Hashimoto, T., Nakamura, N., Shibayama, M., Izumi, A. and Kawai, H. *J. Macromol. Sci., Phys. (B)* 1980, **17**, 389
34 Bates, F. S. and Wignall, G. D. *Phys. Rev. Lett.* 1986, **57**, 1429
35 Sakurai, S., Jinnai, H., Hasegawa, H., Hashimoto, T. and Han, C. C. *Macromolecules* 1991, **24**, 4839
36 Hasegawa, H., Yamasaki, K. and Hashimoto, T. in preparation
37 Stephens, H. L. in 'Polymer Handbook', 3rd Edn. (Eds. J. Brandrup and E. H. Immergut), Wiley, New York, 1989, p. V–1
38 Shafrin, E. G. in 'Polymer Handbook', 2nd Edn. (Eds. J. Brandrup and E. H. Immergut), Wiley, New York, 1975, p. III–221